Effective low-energy theory of graphene in a constant magnetic field

Bachelor Thesis

at the Institute for Theoretical Physics,
Albert Einstein Center for Fundamental Physics,
University of Bern
by

Stephan Caspar

November 2011

Supervisor:
Prof. Dr. Uwe-Jens Wiese
Institute for Theoretical Physics, University of Bern

Abstract

Graphene, a mono-layer of graphite, is a 2D carbon structure, first discovered in 2004 by A. K. Geim and K. S. Novoselov, who received the Nobel prize in 2010. Its geometric structure, the honeycomb-lattice, has already been the subject of theoretical consideration years earlier. Starting from the dispersion relation of a simple tight-binding fermion model, reveals properties of massless Dirac fermions in the region of two points $k_\pm$ in momentum space. We approximate this model at half-filling for low-energy excitations to get correspondence with the Diracian field theory. From the Dirac via the Pauli equation we derive an effective theory for the Dirac quasi-particles in graphene, including interaction with a weak electromagnetic field. Finally, we use this theory to calculate the Landau levels $E_n = \pm v_d\sqrt{2eBn}$ in graphene.

Throughout this paper we use $c = \hbar = 1$.

Contents

1. Introduction

1.1. Historical Aspects

Carbon with its four valence electrons is able to bond in several ways and therefore participates in various structures. This ability made it the most important element in organic chemistry and a requisite for life on earth. Most allotropes of carbon (diamond, graphite, fullerene) where first discovered, before examined theoretically. Graphene, a two-dimensional material with carbon atoms arranged on a honeycomb lattice, instead was first described by P. R. Wallace in 1947 [1], before it was found by K.S. Novoselov and A.K. Geim in 2004 [2]. The description of graphene was only used by Wallace to derive a model for graphite, which can be seen as stacked graphene layers. Graphite was widely known since the invention of the pencil in 1564. In fact the usability of graphite for writing lies in the comparably weak van der Waals coupling between the graphene layers. Wallace, and many others after him, thought that graphene could not exist in its purely two-dimensional form. Until their discovery in 2004, small flat graphene flakes were expected to wrap up and build nanotubes and fullerenes. But Novoselov and Geim were able to consecutively reduce the number of layers in graphite by ripping it apart whit adhesive tape until they finally produced small flakes of single-layer graphene, which were stable at room temperature.

1.2. Properties of graphene

In graphene three electrons participate in sp^2 bonds. These three bonds are realized in a plane with regular 120 angles between them. Each bond is covalently shared with a neighboring atom in a σ-bond, giving graphene its flat hexagonal structure and its robustness. With one electron from each carbon atom all σ-bonds are fully occupied. The fourth valence electron occupies one of two states in the remaining p orbital and forms a half filled π-band. Wallace pointed out that this π-band has no band-gap and an unusual linear dispersion for excited electrons [1]. In neutral graphene (half filling) the Fermi-energy lies exactly at these so-called Dirac points of linear dispersion. This dispersion gives rise to massless Dirac fermions moving with a speed 300 times smaller than the speed of light ($v_D \approx 10^6\, m/s$). Graphene has a very high electron mobility $\approx 250,000\, cm^2/Vs$ combined with a huge carrier density $10^{12}\, cm^{-2}$ resulting in the lowest resistivity ($\approx 10^{-6}\, \Omega\, cm$) of all known materials at room temperature [3].

1.3. Structure and aim of this thesis

This thesis focuses on the electronic properties of graphene only. In section 2 we introduce the conventions and formalism to describe the honeycomb lattice and functions defined on it, as well as intrinsic symmetries of the lattice. We start with a tight binding Hamiltonian in section 3 to describe the electrons in the p orbitals belonging to the π-band. We rediscover the linear dispersion described by Wallace and approximate the dispersion relation and the Hamiltonian at the Fermi energy in terms of the velocity v_D of the Dirac-fermions. On the basis of the approximated Hamiltonian and a form of

the Pauli equation due to Studer and Fröhlich [4] we build up an effective low-energy theory of graphene in section 4, which allows us to couple graphene to an external electromagnetic field and to calculate the corresponding Landau levels. In the last section we briefly recapitulate the result of this thesis and take a look at current researches and possible future applications for graphene.

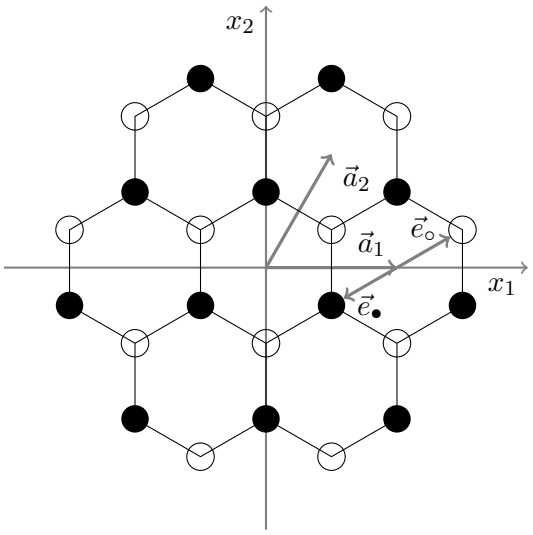

Figure 2.1: Honeycomb lattice with primitive vectors $\vec{a}$ and sublattice vectors $\vec{e}$.

2. The honeycomb lattice

2.1. Geometry of the lattice

Graphen is a two-dimensional carbon-structure, with carbon atoms arranged at the corners of hexagons. This so-called honeycomb lattice itself is not a Bravais lattice, but the centers of each hexagon as well as the $\bullet$- and $\circ$-sublattice form a hexagonal Bravais lattice with the primitive vectors (compare figure 2.1)

$$\vec{a}_1 = d\begin{pmatrix}1\\0\end{pmatrix}, \quad \vec{a}_2 = d\begin{pmatrix}\frac{1}{2}\\\frac{\sqrt{3}}{2}\end{pmatrix}. \tag{2.1}$$

In graphene the lattice constant is $d = 2.46\mathring{A}$ [5], and the distance between to carbon atoms is $a = d/\sqrt{3} = 1.42\mathring{A}$. We now define X as the set of all the vectors on this lattice

$$X := \{\vec{x} \in \mathbb{R}^2 | \vec{x} = n_1\vec{a}_1 + n_2\vec{a}_2,\, n_1, n_2 \in \mathbb{Z}\}. \tag{2.2}$$

The two sublattices $X_\bullet$ and $X_\circ$ can be written as

$$X_\bullet := X + \vec{e}_\bullet = \{\vec{x} \in \mathbb{R}^2 | \vec{x} = n_1\vec{a}_1 + n_2\vec{a}_2 + \vec{e}_\bullet,\, n_1, n_2 \in \mathbb{Z}\},$$

,

$$X_\circ := X + \vec{e}_\circ = \{\vec{x} \in \mathbb{R}^2 | \vec{x} = n_1\vec{a}_1 + n_2\vec{a}_2 + \vec{e}_\circ,\, n_1, n_2 \in \mathbb{Z}\}, \tag{2.3}$$

where we have introduced the sublattice vectors

$$\vec{e}_\circ = -\vec{e}_\bullet = d\begin{pmatrix}\frac{1}{2}\\\frac{\sqrt{3}}{6}\end{pmatrix}. \tag{2.4}$$

2.2. Symmmetries of the lattice

All symmetries of the lattice can be considered as a combination of simple symmetries (D_i, O, R), that we will discuss now shortly.

2.2.1. Shift symmetry D_i

The shift symmetry along a primitive vector $\vec{a}_i$ is a property of any Bravais lattice and therefore of the two sublattices. Since both sublattices have the same primitive vectors the entire honeycomb lattice has this symmetry. The symmetry is given by $\vec{x} \to \vec{x} + \vec{a}_i$. This symmetry maps $\bullet \to \bullet$ and $\circ \to \circ$.

2.2.2. Rotation symmetry O

From figure 2.1 we can see that the honeycomb lattice remains invariant under a rotation by 60°. The symmetry is given by $(x_1, x_2) \to (\frac{1}{2}x_1 - \frac{\sqrt{3}}{2}x_2, \frac{1}{2}x_2 + \frac{\sqrt{3}}{2}x_1)$. This symmetry maps $\bullet \to \circ$ and $\circ \to \bullet$.

2.2.3. Reflection symmetry R

There are several reflection symmetries. We chose the reflection at the x_2-axis, the others can be realised by combining with O. The symmetry is given by $(x_1, x_2) \to (-x_1, x_2)$. This symmetry maps $\bullet \to \bullet$ and $\circ \to \circ$.

2.3. The reciprocal lattice

The reciprocal lattice is defined as all vectors $\vec{k}$ with

$$\forall \vec{x} \in X, \exists n \in \mathbb{Z} : \vec{k} \cdot \vec{x} = 2\pi n. \tag{2.5}$$

The reciprocal primitive vectors $\vec{b}_1, \vec{b}_2$ belonging to $\vec{a}_1, \vec{a}_2$ can be found by the relation

$$\vec{a}_i \cdot \vec{b}_j = 2\pi\delta_{ij}$$

$$\iff \quad \vec{b}_1 = \frac{4\pi}{d\sqrt{3}} \begin{pmatrix} \frac{\sqrt{3}}{2} \\ -\frac{1}{2} \end{pmatrix}, \quad \vec{b}_2 = \frac{4\pi}{d\sqrt{3}} \begin{pmatrix} 0 \\ 1 \end{pmatrix}. \tag{2.6}$$

As before we define K as the set of all the vectors on the reciprocal lattice

$$K := \{\vec{k} \in \mathbb{R}^2 | \vec{k} = n_1\vec{b}_1 + n_2\vec{b}_2,\, n_1, n_2 \in \mathbb{Z}\}. \tag{2.7}$$

2.4. Fourier-transformations

In order to diagonalize the Hamiltonian we will use Fourier-transformations between the $\vec{x}$ and the $\vec{k}$ space. We first define

$$\tilde{f}(\vec{k}) := \sum_{\vec{x} \in X} f_{\vec{x}} \exp(-i\vec{k} \cdot \vec{x}) \tag{2.8}$$

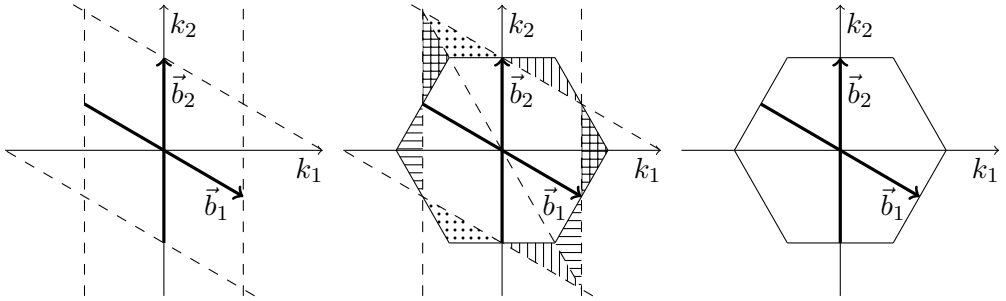

Figure 2.2: Illustration of the relation between the rhombic (left) and the hexagonal (right) Brillouin zone.

for all $\vec{k} \in \mathbb{R}^2$ and operators $f_{\vec{x}} : \mathbb{H} \to \mathbb{H}$ on the Hilbert-space $\mathbb{H}$.
Equation (2.5) states that for all $\vec{k'} \in K$ and $\vec{x} \in X$

$$\exp(i\vec{k'} \cdot \vec{x}) = 1, \tag{2.9}$$

and therefore

$$\tilde{f}(\vec{k}+\vec{k'}) = \sum_{\vec{x}\in X} f_{\vec{x}} \exp(-i(\vec{k}+\vec{k'}) \cdot \vec{x}) = \sum_{\vec{x}\in X} f_{\vec{x}} \exp(-i\vec{k} \cdot \vec{x}) \exp(-i\vec{k'} \cdot \vec{x}) = \tilde{f}(\vec{k}). \tag{2.10}$$

The inverse transformation is an integral over a Brillouin zone $B \subset \mathbb{R}^2$ which fullfills

$$B \oplus K = \{\vec{x} \in \mathbb{R}^2 | \vec{x} = \vec{b} + \vec{k}, \vec{b} \in B, \vec{k} \in K\} = \mathbb{R}^2. \tag{2.11}$$

An intuitive choice is

$$B = \{\vec{k} = m_1\vec{b}_1 + m_2\vec{b}_2 \in \mathbb{R}^2 | -\frac{1}{2} \leq m_1, m_2 < \frac{1}{2}\}. \tag{2.12}$$

Although this Brillouin zone is the handiest for calculations, we rather represent data on a hexagonal Brillouin zone which gives a better impression of the symmetries of the system (the relation between the two Brillouin-zones is shown in figure 2.2).
The inverse Fourier-transformation can be derived from

$$\begin{aligned} f_{\vec{x}} &= \int_{-\frac{1}{2}}^{\frac{1}{2}} dm_1 \int_{-\frac{1}{2}}^{\frac{1}{2}} dm_2 \, \tilde{f}(m_1\vec{b}_1 + m_2\vec{b}_2) \exp(i(m_1\vec{b}_1 + m_2\vec{b}_2) \cdot \vec{x}) \\ &= \frac{\sqrt{3}d^2}{8\pi^2} \int_B d^2k \, \tilde{f}(\vec{k}) \exp(i\vec{k} \cdot \vec{x}). \end{aligned} \tag{2.13}$$

Where we have used

$$k_1 = \frac{2\pi}{d} m_1, \; k_2 = \frac{4\pi}{d\sqrt{3}} \left(-\frac{1}{2} m_1 + m_2 \right) \quad \Longrightarrow \quad m_1 = \frac{d}{2\pi} k_1, \; m_2 = \frac{d\sqrt{3}}{4\pi} k_2 + \frac{d}{4\pi} k_1 \tag{2.14}$$

$$\left| det \frac{\partial(m_1, m_2)}{\partial(k_1, k_2)} \right| = \left| \begin{matrix} \frac{d}{2\pi} & 0 \\ \frac{d}{4\pi} & \frac{d\sqrt{3}}{4\pi} \end{matrix} \right| = \frac{\sqrt{3}d^2}{8\pi^2}. \tag{2.15}$$

We can now identify the δ-functions

$$\delta_{\vec{x},0} = \frac{\sqrt{3}d^2}{8\pi^2} \int_B d^2k \, \exp(i\vec{k} \cdot \vec{x}),$$

$$\delta(\vec{k}) = \frac{\sqrt{3}d^2}{8\pi^2} \sum_{\vec{x}} \exp(-i\vec{k} \cdot \vec{x}). \tag{2.16}$$

3. The tight binding model

In this model electrons are considered to be confined in the attractive potential of an atom. Electrons can then be described by creation and annihilation operators localized at discrete points (the atoms).

3.1. Electron creation and annihilation operators

The electron creation operator is given by $c^\dagger_{x,s}$. It creates an electron at position x with spin $s =\uparrow,\downarrow$. The annihilation operator is given by $c_{x,s}$. These fermion operators obey anti-commutation relations [6]

$$\{c_{x,s}, c^\dagger_{x',s'}\} = \delta_{x,x'}\delta_{s,s'}, \quad \{c_{x,s}, c_{x',s'}\} = 0, \quad \{c^\dagger_{x,s}, c^\dagger_{x',s'}\} = 0, \tag{3.1}$$

implying the Pauli principle (no creation of two electrons in the same state)

$$c^{\dagger 2}_{x,s} = \frac{1}{2}\{c^\dagger_{x,s}, c^\dagger_{x,s}\} = 0. \tag{3.2}$$

We now assume that all states can be obtained by creating electrons from an empty vacuum state $|0\rangle$

$$|\uparrow\rangle_x = c^\dagger_{x,\uparrow}|0\rangle, \quad |\downarrow\rangle_x = c^\dagger_{x,\downarrow}|0\rangle, \quad |\downarrow\uparrow\rangle_x = c^\dagger_{x,\downarrow}c^\dagger_{x,\uparrow}|0\rangle. \tag{3.3}$$

Orthonormality of these states is straightforward to show if we set $\langle 0|0\rangle = 1$.

3.2. Hopping between nearest neighbors

The simplest Hamiltonian in the tight binding model is one that describes hopping of electrons between neighboring sites

$$\mathbb{H} = t \sum_{\langle\vec{x},\vec{y}\rangle,s} \left(c^\dagger_{\vec{x},s} c_{\vec{y},s} + c^\dagger_{\vec{y},s} c_{\vec{x},s} \right), \tag{3.4}$$

where $\langle\vec{x},\vec{y}\rangle$ is a pair of nearest neighbors. Because spin is just an irrelevant summation index we absorb it into

$$c_{\vec{x}} = \begin{pmatrix} c_{\vec{x},\uparrow} \\ c_{\vec{x},\downarrow} \end{pmatrix} \tag{3.5}$$

giving

$$\mathbb{H} = t \sum_{\langle\vec{x},\vec{y}\rangle} \left(c^\dagger_{\vec{x}} c_{\vec{y}} + c^\dagger_{\vec{y}} c_{\vec{x}} \right), \tag{3.6}$$

3.3. Symmetries of the tight binding Hamiltonian

The Hamiltonian inherits all symmetries of the underlying lattice X (D_i, O and R, compare section 2.2) and has symmetries on its own, namely $SU(2)_s$ and $SU(2)_Q$.

3.3.1. Global $SU(2)_s$ and $SU(2)_Q$ symmetries

It is easy to show that

$$\vec{S} = \sum_x c^\dagger_{\vec{x}} \frac{\vec{\sigma}}{2} c_{\vec{x}}, \quad Q^+ = \sum_x (-1)^x c^\dagger_{\vec{x},\uparrow} c^\dagger_{\vec{x},\downarrow}, \quad Q^- = \sum_x (-1)^x c_{\vec{x},\uparrow} c_{\vec{x},\downarrow},$$

$$Q_1 = \frac{1}{2}\left(Q^+ + Q^-\right), \; Q_2 = \frac{i}{2}\left(-Q^+ + Q^-\right), \; Q_3 = \sum_x \frac{1}{2}\left(c_{\vec{x},\uparrow} c_{\vec{x},\uparrow} + c^\dagger_{\vec{x},\downarrow} c^\dagger_{\vec{x},\downarrow} - 1\right) \tag{3.7}$$

all commute with the Hamiltonian $[\mathbb{H}, \vec{S}] = 0$ and $[\mathbb{H}, \vec{Q}] = 0$ ($(-1)^x$ assigns different signs to the sublattices $\circ$ and $\bullet$). Throughout this thesis we use the standard representation of the Pauli matrices

$$\vec{\sigma} = \left(\begin{pmatrix} 0 & 1 \\ 1 & 0 \end{pmatrix}, \begin{pmatrix} 0 & -i \\ i & 0 \end{pmatrix}, \begin{pmatrix} 1 & 0 \\ 0 & -1 \end{pmatrix} \right). \tag{3.8}$$

Here $\vec{S}$ is the generator of the $SU(2)_s$ spin rotation symmetry that implies a unitary operator

$$V = \exp(i\vec{\eta} \cdot \vec{S}), \tag{3.9}$$

which acts on the annihilation operator as

$$c'_{\vec{x}} = V^\dagger c_{\vec{x}} V = \exp(i\vec{\eta} \cdot \frac{\vec{\sigma}}{2}) c_{\vec{x}}. \tag{3.10}$$

This reveals $c_{\vec{x}}$ as an $SU(2)_s$-spinor and makes the Hamiltonian of eq. (3.6) obviously invariant under global $SU(2)_s$ transformations. The relation $[\mathbb{H}, \vec{S}] = 0$ also states that spin is a conserved quantity. The second generator $\vec{Q}$ was first found by Yang and Zhang [7]. Its third component is related to the fermion number operator (with respect to half filling) as $Q_3 = \frac{1}{2}Q$, which makes $SU(2)_Q$ an extension of the $U(1)_Q$ symmetry well known from electrodynamics. Similar to spin rotation there exists a fermion number spinor

$$d_{\vec{x}} = \begin{pmatrix} c_{\vec{x},\uparrow} \\ (-1)^x c^\dagger_{\vec{x},\downarrow} \end{pmatrix} \tag{3.11}$$

and a unitary operator

$$W = \exp(i\vec{\omega} \cdot \vec{Q}), \tag{3.12}$$

acting on it as (here $\vec{\sigma}$ acts in the fermion number Hilbert space)

$$d'_{\vec{x}} = W^\dagger d_{\vec{x}} W = \exp(i\vec{\omega} \cdot \frac{\vec{\sigma}}{2}) d_{\vec{x}}. \tag{3.13}$$

Using $d_{\vec{x}}$ we can rewrite the generator $\vec{Q}$ as

$$\vec{Q} = \sum_x d^\dagger_{\vec{x}} \frac{\vec{\sigma}}{2} d_{\vec{x}} \tag{3.14}$$

and the Hamiltonian of eq. (3.4) as

$$\mathbb{H} = t \sum_{\langle \vec{x},\vec{y} \rangle} \left(d^\dagger_{\vec{x}} d_{\vec{y}} + d^\dagger_{\vec{y}} d_{\vec{x}} \right), \tag{3.15}$$

which is obviously invariant under $SU(2)_Q$ transformations. Again $[\mathbb{H}, \vec{Q}] = 0$ implies charge respectively fermion number conservation. The extension of $U(1)_Q$ to $SU(2)_Q$ predicts a symmetry between electrons and holes, and will be explicitly broken by adding next-to-nearest neighbor hopping (compare section 3.7). Neither eq. (3.6) nor eq. (3.15) is obviously $SU(2)_s \otimes SU(2)_Q$ invariant. There exists a representation with a matrix operator instead of spinors, which has this property. A detailed construction of this representation can be found in [8].

3.4. Solutions of the tight binding Hamiltonian

Using the definitions of the lattice, the tight binding Hamiltonian can be written as

$$\begin{aligned} \mathbb{H} = t \sum_{\vec{x} \in X} \Big(& c^\dagger_{\vec{x}+\vec{e}_\bullet+\vec{a}_1} c_{\vec{x}+\vec{e}_\circ} + c^\dagger_{\vec{x}+\vec{e}_\circ} c_{\vec{x}+\vec{e}_\bullet+\vec{a}_2} + c^\dagger_{\vec{x}+\vec{e}_\bullet+\vec{a}_2} c_{\vec{x}+\vec{e}_\circ-\vec{a}_1} \\ & + c^\dagger_{\vec{x}+\vec{e}_\circ-\vec{a}_1} c_{\vec{x}+\vec{e}_\bullet} + c^\dagger_{\vec{x}+\vec{e}_\bullet} c_{\vec{x}+\vec{e}_\circ-\vec{a}_2} + c^\dagger_{\vec{x}+\vec{e}_\circ-\vec{a}_2} c_{\vec{x}+\vec{e}_\bullet+\vec{a}_1} \Big). \end{aligned} \tag{3.16}$$

The hopping parameter in graphene takes the value $t = 2.8\,eV$ [5]. The D_i invariance discussed before implies a conserved lattice momentum $\vec{k}$. In order to rewrite the Hamiltonian in the $\vec{k}$-basis we have to apply a Fourier-transformation to the operators. The Fourier-transformed annihilation operators are given by

$$\tilde{c}_\bullet(\vec{k}) = \sum_{\vec{x} \in X_\bullet} c_{\vec{x}} \exp(-i\vec{k} \cdot \vec{x}), \quad \tilde{c}_\circ(\vec{k}) = \sum_{\vec{x} \in X_\circ} c_{\vec{x}} \exp(-i\vec{k} \cdot \vec{x}), \tag{3.17}$$

and the inverse transformations are given by

$$\begin{aligned} c_{\vec{x}+\vec{e}_\bullet} &= \frac{\sqrt{3}d^2}{8\pi^2} \int_B d^2k\, \tilde{c}_\bullet(\vec{k}) \exp(i\vec{k} \cdot (\vec{x} + \vec{e}_\bullet)), \\ c_{\vec{x}+\vec{e}_\circ} &= \frac{\sqrt{3}d^2}{8\pi^2} \int_B d^2k\, \tilde{c}_\circ(\vec{k}) \exp(i\vec{k} \cdot (\vec{x} + \vec{e}_\circ)) \end{aligned} \tag{3.18}$$

Inserting these into the Hamiltonian we arrive at (for step by step calculations compare appendix A)

$$\mathbb{H} = t \left(\frac{\sqrt{3}d^2}{8\pi^2} \right) \int_B d^2k \begin{pmatrix} \tilde{c}^\dagger_\bullet & \tilde{c}^\dagger_\circ \end{pmatrix} \begin{pmatrix} 0 & g^* \\ g & 0 \end{pmatrix} \begin{pmatrix} \tilde{c}_\bullet \\ \tilde{c}_\circ \end{pmatrix}, \tag{3.19}$$

where we have introduced the phase factor

$$g(\vec{k}) := \Big(\exp(i\vec{k} \cdot \vec{a}_1) + \exp(i\vec{k} \cdot \vec{a}_2) + \exp(i\vec{k} \cdot (\vec{a}_1 + \vec{a}_2)) \Big) \exp(i2\vec{k} \cdot \vec{e}_\bullet). \tag{3.20}$$

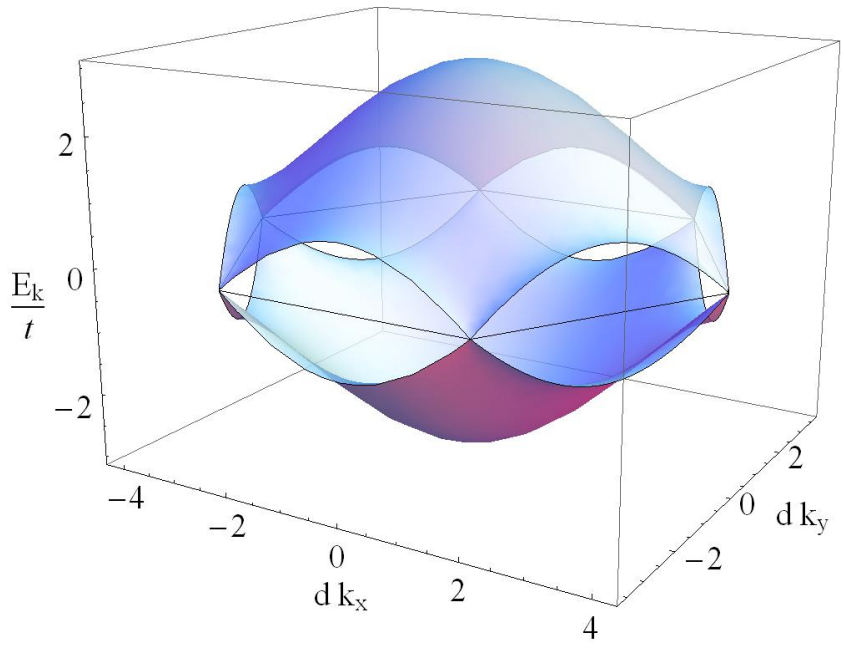

Figure 3.1: Dispersion relation on the hexagonal Brillouin zone (only nearest neighbor coupling, next-to-nearest neighbor coupling is illustrated in figure 3.3).

A unitary transformation yields diagonalisation of this matrix ($g = |g|e^{i\alpha}$)

$$U := \frac{1}{\sqrt{2}} \begin{pmatrix} e^{i\frac{\alpha}{2}} & e^{-i\frac{\alpha}{2}} \\ e^{i\frac{\alpha}{2}} & -e^{-i\frac{\alpha}{2}} \end{pmatrix} \quad U^\dagger U = 1 \Longrightarrow \tag{3.21}$$

$$U \begin{pmatrix} 0 & g^* \\ g & 0 \end{pmatrix} U^\dagger = \frac{1}{2} \begin{pmatrix} e^{i\frac{\alpha}{2}} & e^{-i\frac{\alpha}{2}} \\ e^{i\frac{\alpha}{2}} & -e^{-i\frac{\alpha}{2}} \end{pmatrix} \begin{pmatrix} g^* e^{i\frac{\alpha}{2}} & -g^* e^{i\frac{\alpha}{2}} \\ g e^{-i\frac{\alpha}{2}} & g e^{-i\frac{\alpha}{2}} \end{pmatrix} = \begin{pmatrix} |g| & 0 \\ 0 & -|g| \end{pmatrix} \tag{3.22}$$

and therefore the Hamiltonian in diagonal form

$$\mathbb{H} = t \left(\frac{\sqrt{3}d^2}{8\pi^2} \right) \int_B d^2k \begin{pmatrix} \tilde{c}^\dagger_{s,\bullet} & \tilde{c}^\dagger_{s,\circ} \end{pmatrix} U^\dagger \begin{pmatrix} |g| & 0 \\ 0 & -|g| \end{pmatrix} U \begin{pmatrix} \tilde{c}_{s,\bullet} \\ \tilde{c}_{s,\circ} \end{pmatrix}. \tag{3.23}$$

The possible energy-eigenvalues are given by

$$E_\pm(\vec{k}) = \pm t|g(\vec{k})|. \tag{3.24}$$

3.5. Dirac cones

We have seen in section 3.2 that the energy of an electron mode is governed by the function $|g(\vec{k})|$, with a symmetry between positive and negative energy eigenstates. We will see that this symmetry does not hold when we consider hopping to next-to-nearest

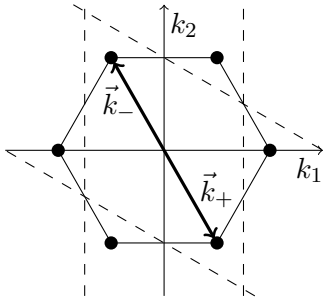

Figure 3.2: Position of the spots with $|g| = 0$ and justification of the hexagonal Brillouin-zone.

neighbors (compare section 3.7). We now take a closer look at the dependency of $|g|$ on $\vec{k}$. We see that the negative and positive energy states meet only at the two distinct points

$$\vec{k}_\pm = \pm\frac{4\pi}{d\sqrt{3}}\begin{pmatrix}\frac{\sqrt{3}}{6}\\ -\frac{1}{2}\end{pmatrix}, \tag{3.25}$$

which are exactly the edges of the hexagonal Brillouin zone (see figure 3.2). Since at half-filling all low-energy excitations will be in this lattice momentum region we focus on an expansion of $|g|$ in terms of small relative deviation $\Delta\vec{k}$ from $\vec{k}_\pm$. The quantity $|g|$ as a function of k_1 and k_2 takes the form

$$|g(\vec{k})| = \sqrt{3 + 2\cos(dk_1) + 4\cos(\frac{d}{2}k_1)\cos(\frac{d\sqrt{3}}{2}k_2)}, \tag{3.26}$$

and can be expanded around $\vec{k}_\pm$ as ($\Delta k_1 = \Delta k\cos(\alpha)$,$\Delta k_2 = \Delta k\sin(\alpha)$, detailed calculation can be found in appendix B.1)

$$|g(\vec{k}_\pm + \Delta\vec{k})| = \frac{\sqrt{3}d}{2}\Delta k \mp \frac{d^2}{8}\cos(3\alpha)\Delta k^2 + \mathcal{O}(\Delta k^3). \tag{3.27}$$

The dispersion relation becomes

$$E_\pm(\vec{k}_\pm + \Delta\vec{k}) = \pm\frac{\sqrt{3}dt}{2}\Delta k + \mathcal{O}(\Delta k^2), \tag{3.28}$$

which implies phase and group velocity given by the Dirac velocity

$$\frac{dE}{d\Delta k} = \frac{E}{\Delta k} = v_D = \frac{\sqrt{3}dt}{2} \tag{3.29}$$

for energies around $E = 0$. This is a behavior we know from massless particles such as photons where the energy is given by $E(\vec{p}) = p$, only here with reduced speed v_D

$$E(\Delta\vec{k}) = \Delta k\, v_D. \tag{3.30}$$

3.6. Expansion of the Hamiltonian for $E \approx 0$

Another way to obtain the result above is to expand the Hamiltonian in a series around $\vec{k}_\pm$ (detailed calculations can be found in appendix B.2)

$$g(\vec{k}_\pm + \Delta\vec{k}) = \frac{\sqrt{3}d}{2}\begin{pmatrix}\pm 1 & i\end{pmatrix}\begin{pmatrix}\cos(\frac{4\pi}{3}) & -\sin(\frac{4\pi}{3})\\ \sin(\frac{4\pi}{3}) & \cos(\frac{4\pi}{3})\end{pmatrix}\begin{pmatrix}\Delta k_1\\ \Delta k_2\end{pmatrix} + \mathcal{O}(\Delta k_i^2). \tag{3.31}$$

Choosing a new basis p_1, p_2 rotated by an angle $\frac{4\pi}{3}$ with respect to $\Delta k_1, \Delta k_2$ yields

$$g_\pm(\vec{p}) = \frac{\sqrt{3}d}{2}\left(\pm p_1 + i p_2\right). \tag{3.32}$$

Inserting this into equation (3.19) gives

$$\mathbb{H}_\pm = v_D\left(\frac{\sqrt{3}d^2}{8\pi^2}\right)\int_B d^2p\begin{pmatrix}\tilde{c}_\bullet^\dagger & \tilde{c}_\circ^\dagger\end{pmatrix}\begin{pmatrix}0 & \pm p_1 - i p_2\\ \pm p_1 + i p_2 & 0\end{pmatrix}\begin{pmatrix}\tilde{c}_\bullet\\ \tilde{c}_\circ\end{pmatrix} \tag{3.33}$$

where we recognize the Dirac Hamiltonian

$$\mathbb{H}_\pm = v_D\left(\pm\sigma_1 p_1 + \sigma_2 p_2\right) \tag{3.34}$$

with v_D instead of the velocity of light and $m = 0$. For further convenience we introduce the 2D γ-matrices

$$\vec{\gamma}_\pm = \left(\pm\begin{pmatrix}0 & 1\\ 1 & 0\end{pmatrix}, \begin{pmatrix}0 & -i\\ i & 0\end{pmatrix}\right) \tag{3.35}$$

to distinguish between the operator $\vec{\sigma}$ (which acts on the spin spinor $(\uparrow,\downarrow)$) and $\vec{\gamma}$ (which acts on the sublattice spinor $(\bullet,\circ)$). The Hamiltonian can then be written as

$$\mathbb{H}_\pm = v_D \gamma_\pm^i p_i. \tag{3.36}$$

Applying it twice

$$\mathbb{H}_\pm^2 = v_D^2\left(p_1^2 + p_2^2\right) = v_D^2\,\vec{p}^{\,2} \tag{3.37}$$

gives us the same dispersion relation as above

$$E_\pm(\vec{p}) = \pm v_D|\vec{p}|. \tag{3.38}$$

3.7. Stability of the Dirac cones

We want to see whether the Dirac cones discovered in the previous section are really a property of graphene and the honeycomb lattice and not only a curiosity of our model. Therefore we add a second term to our Hamiltonian defined in eq. (3.4), which describes hopping between next-to-nearest neighbors, i.e. hopping on one of the sublattices

$$\begin{aligned}\mathbb{H}_1 := t'\sum_{\vec{x}}\Big(&c^\dagger_{\vec{x}+\vec{e}_\bullet}c_{\vec{x}+\vec{e}_\bullet+\vec{a}_1} + c^\dagger_{\vec{x}+\vec{e}_\bullet+\vec{a}_1}c_{\vec{x}+\vec{e}_\bullet+\vec{a}_2} + c^\dagger_{\vec{x}+\vec{e}_\bullet+\vec{a}_2}c_{\vec{x}+\vec{e}_\bullet}\\ &+c^\dagger_{\vec{x}+\vec{e}_\bullet+\vec{a}_1}c_{\vec{x}+\vec{e}_\bullet} + c^\dagger_{\vec{x}+\vec{e}_\bullet+\vec{a}_2}c_{\vec{x}+\vec{e}_\bullet+\vec{a}_1} + c^\dagger_{\vec{x}+\vec{e}_\bullet}c_{\vec{x}+\vec{e}_\bullet+\vec{a}_2}\\ &+c^\dagger_{\vec{x}+\vec{e}_\circ}c_{\vec{x}+\vec{e}_\circ-\vec{a}_1} + c^\dagger_{\vec{x}+\vec{e}_\circ-\vec{a}_1}c_{\vec{x}+\vec{e}_\circ-\vec{a}_2} + c^\dagger_{\vec{x}+\vec{e}_\circ-\vec{a}_2}c_{\vec{x}+\vec{e}_\circ}\\ &+c^\dagger_{\vec{x}+\vec{e}_\circ-\vec{a}_1}c_{\vec{x}+\vec{e}_\circ} + c^\dagger_{\vec{x}+\vec{e}_\circ-\vec{a}_2}c_{\vec{x}+\vec{e}_\circ-\vec{a}_1} + c^\dagger_{\vec{x}+\vec{e}_\circ}c_{\vec{x}+\vec{e}_\circ-\vec{a}_2}\Big)\end{aligned} \tag{3.39}$$

with the hopping parameter bounded by $0.02t \leq t' \leq 0.2t$ (this range was obtained by fitting a third-nearest tight-binding model to experimental results [9]). Repeating the steps from before one reaches

$$\mathbb{H}_1 = t' \left(\frac{\sqrt{3}d^2}{8\pi^2} \right) \int_B d^2k \Big(h(\vec{k})\, \tilde{c}_\bullet(\vec{k})^\dagger \tilde{c}_\bullet(\vec{k}) + h(\vec{k})\, \tilde{c}_\circ(\vec{k})^\dagger \tilde{c}_\circ(\vec{k}) \Big). \tag{3.40}$$

With the new phase factor

$$\begin{aligned} h(\vec{k}) :=& \exp(i\vec{k}\cdot\vec{a}_1) + \exp(i\vec{k}\cdot(\vec{a}_2 - \vec{a}_1)) + \exp(-i\vec{k}\cdot\vec{a}_2) \\ &+ \exp(-i\vec{k}\cdot\vec{a}_1) + \exp(-i\vec{k}\cdot(\vec{a}_2 - \vec{a}_1)) + \exp(i\vec{k}\cdot\vec{a}_2) \\ =& 2\cos(\vec{k}\cdot\vec{a}_1) + 2\cos(\vec{k}\cdot(\vec{a}_2 - \vec{a}_1)) + 2\cos(\vec{k}\cdot\vec{a}_2). \end{aligned} \tag{3.41}$$

Added to the Hamiltonian from eq. (3.19) this takes the form

$$\mathbb{H} + \mathbb{H}_1 = \left(\frac{\sqrt{3}d^2}{8\pi^2} \right) \int_B d^2k \begin{pmatrix} \tilde{c}_\bullet^\dagger & \tilde{c}_\circ^\dagger \end{pmatrix} \begin{pmatrix} ht' & g^*t \\ gt & ht' \end{pmatrix} \begin{pmatrix} \tilde{c}_\bullet \\ \tilde{c}_\circ \end{pmatrix}. \tag{3.42}$$

The same unitary transformation yields diagonalisation

$$\mathbb{H} + \mathbb{H}_1 = \left(\frac{\sqrt{3}d^2}{8\pi^2} \right) \int_B d^2k \begin{pmatrix} \tilde{c}_\bullet^\dagger & \tilde{c}_\circ^\dagger \end{pmatrix} U^\dagger \begin{pmatrix} ht' + |g|t & 0 \\ 0 & ht' - |g|t \end{pmatrix} U \begin{pmatrix} \tilde{c}_\bullet \\ \tilde{c}_\circ \end{pmatrix}. \tag{3.43}$$

Remembering eq. (3.26) one finds

$$h(\vec{k}) = |g(\vec{k})|^2 - 3. \tag{3.44}$$

And from eq. (3.27)

$$h(\vec{k}_\pm + \Delta\vec{k}) = -3 + \frac{3}{4} d^2 \Delta k^2 + \mathcal{O}(\Delta k^3), \tag{3.45}$$

The new dispersion relation then becomes

$$E(\vec{k}_\pm + \Delta\vec{k}) = -3t' + \frac{\sqrt{3}dt}{2}\Delta k + \left(\frac{3}{4} d^2 t' \mp \frac{d^2 t}{8} \cos(3\alpha) \right) \Delta k^2 + \mathcal{O}(\Delta k^3). \tag{3.46}$$

With t' considered to be much smaller than t, this gives only a small shift of the energy in the region of the Dirac cones but the linear approximation itself holds (compare figure 3.3). Adding $\mathbb{H}_1$ explicitly breaks $SU(2)_Q$ to its subgroup $U(1)_Q$, since $[\mathbb{H}_1, \vec{Q}] \neq 0$ but still $[\mathbb{H}_1, Q] = 0$. As we can see in eq. (3.46) this breaks the symmetry between electrons and holes (even when neglecting the $-3t'$ shift). The commutation relation $[\mathbb{H}_1, \vec{S}] = 0$ is still valid, so $SU(2)_s \otimes U(1)_Q$ remains a microscopic symmetry of graphene.

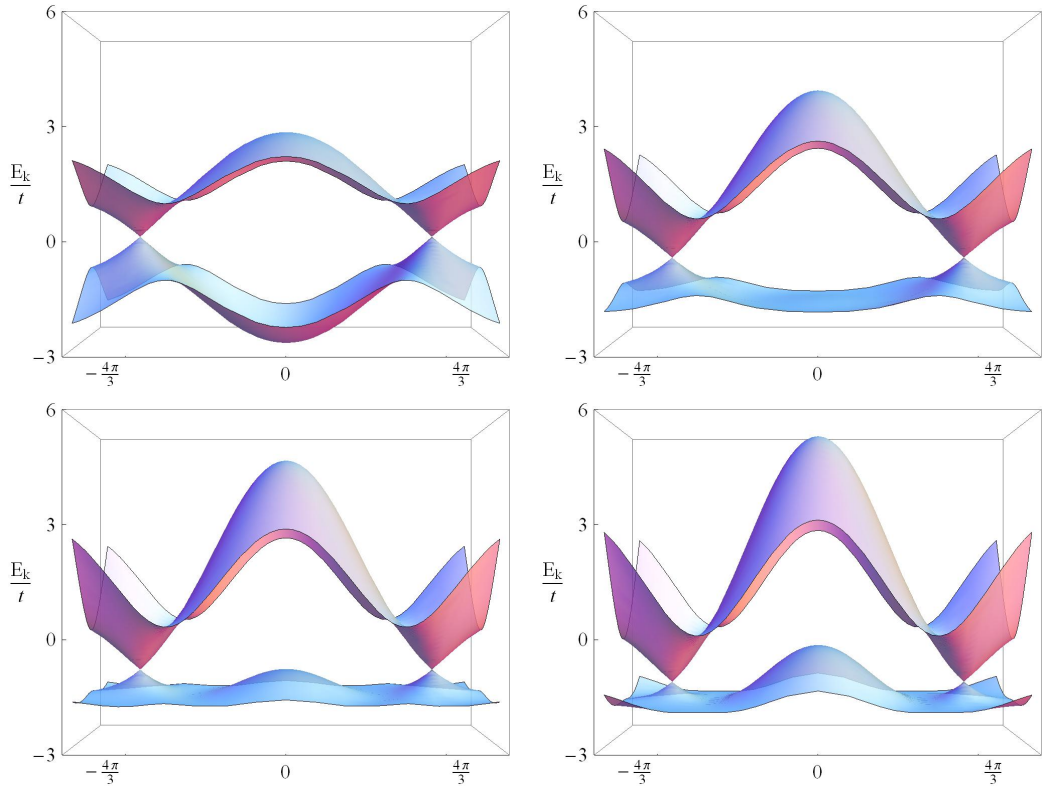

Figure 3.3: Dependence of the dispersion relation on the parameter t' (for $t'/t = 0, 0.2, 0.33, 0.45$). Notice the stability of the Dirac cones up to the $-3t'$ shift, the asymmetry of valence and conduction band (except for $t' = 0$) and the displacement of the Fermi energy from the Dirac points for $t' > t/3$ (existence of valence band states with higher energy than conduction band states).

4. Effective low-energy theory of graphene

4.1. Local $SU(2)_s \otimes U(1)_Q$ spin symmetric form of the Pauli equation

We want to derive a macroscopic field theory for graphene from the microscopic tight binding model. We start with the Pauli equation, which describes non-relativistic electrons (which our Dirac-like electrons with velocity v_D actually are). Studer and Fröhlich [4] observed that the Pauli equation has (up to corrections of order m^{-3}) an even local $SU(2)_s \otimes U(1)_Q$ symmetry. The Pauli equation then takes the form

$$i\left(\partial_t - ie\Phi + i\frac{e}{8m^2}\vec{\nabla}\cdot\vec{E} + i\frac{e}{2m}\vec{B}\cdot\vec{\sigma}\right)\Psi = -\frac{1}{2m}\left(\vec{\nabla} + ie\vec{A} - i\frac{e}{4m}\vec{E}\times\vec{\sigma}\right)^2\Psi, \quad (4.1)$$

which can also be written with covariant derivatives

$$iD_t\Psi = -\frac{1}{2m}D_iD_i\Psi. \quad (4.2)$$

In this case the $SU(2)_s \otimes U(1)_Q$ covariant derivatives are given by

$$D_\mu = \partial_\mu + W_\mu + ieA_\mu. \quad (4.3)$$

We can identify the $U(1)_Q$ vector potential A_μ well-known from electrodynamics, except for a small deviation by the Darwin correction in its time component

$$A_t = -\Phi + \frac{1}{8m^2}\vec{\nabla}\cdot\vec{E}. \quad (4.4)$$

The non-Abelian vector potential of $SU(2)_s$ is given by

$$W_\mu = iW_\mu^a\frac{\sigma_a}{2} \quad (4.5)$$

and

$$W_t^a = \frac{e}{m}B^a, \quad W_i^a = \frac{e}{2m}\epsilon_{iab}E^b. \quad (4.6)$$

A detailed analysis of the properties of these covariant derivatives was made in [10]. In eq. (4.2) we identify the underlying equation for free non-relativistic electrons ($\vec{A} = 0, \Phi = 0$)

$$i\partial_t\Psi = -\frac{1}{2m}\partial^i\partial_i = -\frac{1}{2m}\Delta\Psi. \quad (4.7)$$

In analogy to this, we can replace in our quasi Dirac equation

$$i\partial_t\Psi = -iv_D\gamma_\pm^i\partial_i\Psi \quad (4.8)$$

the derivatives ∂_μ by their $SU(2)_s \otimes U(1)_Q$ covariant derivatives D_μ

$$iD_t\Psi = -iv_D\gamma_\pm^iD_i\Psi \quad (4.9)$$

providing the coupling of electromagnetic fields to the graphene electrons

$$i\left(\partial_t - ie\Phi + i\frac{e}{8m^2}\partial_i E^i + i\frac{e}{2m}\sigma_i B^i\right)\Psi = -iv_D\,\gamma_\pm^i\left(\partial_i + ieA_i - i\frac{e}{4m}\epsilon_{ijk}E^j\sigma^k\right)\Psi. \tag{4.10}$$

At this point one has to take into consideration, that we are working with an equation for a (sublattice-) pseudo spinor. The operator $\vec{\gamma}$ acts on this spinor, while $\vec{\sigma}$ acts on the absorbed spin in each component of the (sublattice-) spinor (compare eq. (3.5). We could solve this by introducing a four-spinor and replacing $\vec{\gamma}$ and $\vec{\sigma}$ accordingly. However, Gusynin and Sharapov [11] pointed out that all terms of order m^{-1} (Zeeman effect and spin-orbit coupling) and higher can be neglected in the low-energy regime where (4.8) is valid. This leaves the effective theory as we are going to use it

$$i\left(\partial_t - ie\Phi\right)\Psi = -iv_D\,\gamma_\pm^i\left(\partial_i + ieA_i\right)\Psi, \tag{4.11}$$

where the spin does not appear explicitly and can therefore be treated like a flavor degree of freedom.

4.2. Landau levels in graphene

As we have seen before, the effective Hamiltonian can be written as

$$\mathbb{H}_\pm = -iv_D\,\gamma_\pm^i\left(\partial_i + ieA_i\right) - e\Phi. \tag{4.12}$$

In oder to calculate the Landau-levels we apply a constant magnetic field $\vec{B} = (0, 0, B)$, and a corresponding vector potential $\vec{A} = (0, Bx, 0)$, $\Phi = 0$. We can then rewrite eq. (4.12) as a time independent Hamiltonian

$$\mathbb{H}_\pm = -iv_D\left[\gamma_\pm^x\partial_x + \gamma_\pm^y(\partial_y + ieBx)\right] \tag{4.13}$$

which is invariant under translations in the y-direction. Therefore we can apply Fourier-transformation to the equation in this direction

$$\mathbb{H}_\pm = -iv_D\left[\gamma_\pm^x\partial_x + \gamma_\pm^y(ik_y + ieBx)\right], \tag{4.14}$$

and substitution of x by $\xi = \sqrt{eB}(x + \frac{k_y}{eB})$ gives

$$\mathbb{H}_\pm = v_D\sqrt{eB}\left[-i\gamma_\pm^x\partial_\xi + \gamma_\pm^y\xi\right]. \tag{4.15}$$

Rewriting this equation in matrix form

$$\mathbb{H}_\pm = v_D\sqrt{eB}\begin{pmatrix} 0 & \mp i\partial_\xi - i\xi \\ \mp i\partial_\xi + i\xi & 0 \end{pmatrix}, \tag{4.16}$$

and substituting with $a_\pm = (\xi \pm \partial_\xi)/\sqrt{2}$, we obtain

$$\mathbb{H}_\pm = v_D\sqrt{2eB}\begin{pmatrix} 0 & -ia_\pm \\ ia_\pm^\dagger & 0 \end{pmatrix}. \tag{4.17}$$

The operators $a = a_+ = a_-^\dagger$ ($a^\dagger = a_+^\dagger = a_-$) we know very well as the anihilation (creation) operators of the harmonic oscillator ($\omega = 1$) [12]

$$\mathbb{H}_{osc} = -\frac{1}{2}\partial_\xi^2 + \frac{1}{2}\xi^2 = N + \frac{1}{2}, \quad N = a^\dagger a, \quad [a, a^\dagger] = 1, \tag{4.18}$$

which is in our definition

$$a_\pm^\dagger a_\pm = N + \frac{1}{2} \mp \frac{1}{2}, \quad [a_\pm, a_\pm^\dagger] = \pm 1. \tag{4.19}$$

The square of eq. (4.17) is

$$\begin{aligned}\mathbb{H}_\pm^2 &= v_D^2 2eB \begin{pmatrix} a_\pm a_\pm^\dagger & 0 \\ 0 & a_\pm^\dagger a_\pm \end{pmatrix} = v_D^2 eB \begin{pmatrix} 2N+1\pm 1 & 0 \\ 0 & 2N+1\mp 1 \end{pmatrix} \\ &= v_D^2 eB(2N + 1 \pm \sigma^z) = v_D^2 eB(2N + 1 + \sigma_\pm^3).\end{aligned} \tag{4.20}$$

Since $\mathbb{H}_\pm^2$ has eigenvalues $v_D^2 2eBn, n \in \mathbb{N}$, all possible eigenvalues of $\mathbb{H}_+$ (and $\mathbb{H}_-$) are given by $\pm v_D\sqrt{2eBn}, n \in \mathbb{N}$. In order to prevent confusion between $\pm$ as an index for the Dirac points and $\pm$ as an indication of the positive and negative energy values we continue our calculations only with $\mathbb{H}_+$. All results are also valid for $\mathbb{H}_-$. We will see that there are eigenvectors to all possible eigenvalues. However, first we take a look at the eigenfunctions of N

$$\varphi_0 = \left(\frac{1}{\pi}\right)^{1/4} \exp(-\frac{\xi^2}{2}), \quad \varphi_n = \frac{1}{\sqrt{n!}}(a^\dagger)^n \varphi_0 : \tag{4.21}$$

The operators act on them as

$$N\varphi_n = n\varphi_n, \quad a\varphi_n = \sqrt{n}\varphi_{n-1}, \quad a^\dagger\varphi_n = \sqrt{n+1}\varphi_{n+1}. \tag{4.22}$$

It is straightforward to show that the eigenfunctions to the energy values $E_n^\pm = \pm v_D\sqrt{2eBn}$ are

$$\psi_0(\xi) = \begin{pmatrix} 0 \\ \varphi_0(\xi) \end{pmatrix}, \quad \psi_n^\pm(\xi) = \frac{1}{\sqrt{2}} \begin{pmatrix} \varphi_{n-1}(\xi) \\ \pm i\varphi_n(\xi) \end{pmatrix}. \tag{4.23}$$

5. Conclusion and outlook

5.1. Recapitulation

We started with a discussion of the honeycomb lattice, which we found not to be a Bravais lattice itself, but could be viewed as a combination of two hexagonal sublattices (∘,•) . On this lattice we established a tight-binding model (localized electrons hopping from site to site) which featured Dirac cones $E(\Delta\vec{k}) = \pm v_D \Delta k$ around the two Dirac points $\vec{k}_\pm$. We showed that the cones and the velocity are unaffected by next-to-nearest neighbor hopping effects and that the Fermi-energy at half filling (neutral graphene) lies exactly at the Dirac points. We combined the linear dispersion and the $SU(2)_s \otimes U(1)_Q$ microscopic symmetry with the Pauli equation of Studer and Fröhlich to an effective low-energy theory of graphene, given by $iD_t\Psi = -iv_D\gamma^i_\pm D_i\Psi$ (where D_μ are the $SU(2)_s \otimes U(1)_Q$ covariant derivatives). This allowed us to calculate the Landau-levels $E_n = \pm v_D\sqrt{2eBn}$ in graphene.

5.2. Conclusions

We saw that we are able to derive electronic properties of a material by simple analysis of its geometry. The rise of massless Dirac fermions in graphene follows directly from its double hexagonal lattice structure. Since the lower (valence-band, filled) and upper (conduction-band, empty) half of the energy spectrum are only connected at the Dirac points, we expect graphene to have semi-metallic properties. Because of the minimal connection of the two bands (the state density goes to zero at the Dirac points) graphene could also be called a zero-gap semiconductor. It has already been shown that graphene can be turned into a semiconductor (with gap) by connection to other electronic materials or external fields. Even full control over the electronic properties (switch between metallic and semiconductor) seems likely.

5.3. Outlook

The number of imagined applications is increasing ever since the discovery of graphene. The main goal is to use graphene in electronics. By controlling its semiconductor properties, graphene could become a competitor of silicon based transistors and capacities. Its thinness of one atom size could reduce size - high drift velocity, large carrier concentration, sustainability for high currents and long scattering distance at room temperature could improve signal transport and electricity consumption - and the quantum effects present in graphene at high temperature even shed light on new applications in most electronic devices. Because of its high permeability for light, its mechanical flexibility and high breaking strength it could also be interesting in optical devices such as touch- and bendable screens or photoelectric cells. The electronic properties of graphene have been studied very carefully and comprehensively. Less known are its mechanical and thermodynamical properties, mainly due to problems in modeling such systems and the absence of cheap graphene samples to experiment with. Huge progress was made in the theoretical understanding of graphene since its discovery, but the main problem remains:

fabrication. The original drawing or scotch tape method is not expected to produce large size samples of monolayer graphene. Epitaxial growth on different substrates like silicon carbide, ruthenium, iridium or copper from liquid or vapor are the subject of current research. They all struggle with difficulties in temperature/pressure control, impurity and strong dependence on the substrate. Still, production of large size samples seams possible. Another huge problem especially in electronic applications is atomic size customization of graphene. Appropriate tools for producing and testing samples to atomic precision are lacking [3]. Nevertheless graphene seems to be one of the most promising new materials and will be subject of intensive research in the following years.

Acknowledgments

Special thanks go to Professor Uwe-Jens Wiese, who's lectures inspired me for a bachelor thesis in theoretical physics in the first place. I would like to thank him for his support and supervision during the development of this thesis.

I am also grateful to my collaborators Carla Gross and Sacha Schwarz. Their views on the subject widened my perspective and kept me from wrong tracks. I am looking forward to working with them again.

A. Diagonalisation of the Hamiltonian

Inserting the $\vec{k}$-basis operators into eq. (3.16) we get

$$\begin{aligned}\mathbb{H} = t\sum_{\vec{x}}\left(\frac{\sqrt{3}d^2}{8\pi^2}\right)^2 \int_B d^2k \int_{B'} d^2k' \\ \Big(\tilde{c}_\bullet(\vec{k})^\dagger \tilde{c}_\circ(\vec{k}')\exp(i(\vec{k}'\cdot(\vec{x}+\vec{e}_\circ) - \vec{k}\cdot(\vec{x}+\vec{e}_\bullet+\vec{a}_1))) \\ + \tilde{c}_\bullet(\vec{k})^\dagger \tilde{c}_\circ(\vec{k}')\exp(i(\vec{k}'\cdot(\vec{x}+\vec{e}_\circ-\vec{a}_1) - \vec{k}\cdot(\vec{x}+\vec{e}_\bullet+\vec{a}_2))) \\ + \tilde{c}_\bullet(\vec{k})^\dagger \tilde{c}_\circ(\vec{k}')\exp(i(\vec{k}'\cdot(\vec{x}+\vec{e}_\circ-\vec{a}_2) - \vec{k}\cdot(\vec{x}+\vec{e}_\bullet))) + h.c.\Big),\end{aligned} \tag{A.1}$$

where we can identify the δ-function $\delta(\vec{k}-\vec{k}')$

$$\begin{aligned}\mathbb{H} = t\left(\frac{\sqrt{3}d^2}{8\pi^2}\right) \int_B d^2k \int_{B'} d^2k'\,\delta(\vec{k}-\vec{k}') \\ \Big(\tilde{c}_\bullet(\vec{k})^\dagger \tilde{c}_\circ(\vec{k}')\exp(i(\vec{k}'\cdot\vec{e}_\circ - \vec{k}\cdot(\vec{e}_\bullet+\vec{a}_1))) \\ + \tilde{c}_\bullet(\vec{k})^\dagger \tilde{c}_\circ(\vec{k}')\exp(i(\vec{k}'\cdot(\vec{e}_\circ-\vec{a}_1) - \vec{k}\cdot(\vec{e}_\bullet+\vec{a}_2))) \\ + \tilde{c}_\bullet(\vec{k})^\dagger \tilde{c}_\circ(\vec{k}')\exp(i(\vec{k}'\cdot(\vec{e}_\circ-\vec{a}_2) - \vec{k}\cdot\vec{e}_\bullet)) + h.c.\Big).\end{aligned} \tag{A.2}$$

Integrating over $\vec{k}'$ gives

$$\begin{aligned}\mathbb{H} = t\left(\frac{\sqrt{3}d^2}{8\pi^2}\right) \int_B d^2k\,\tilde{c}_\bullet(\vec{k})^\dagger \tilde{c}_\circ(\vec{k})\Big(\exp(i\vec{k}\cdot(\vec{e}_\circ-\vec{e}_\bullet-\vec{a}_1)) \\ + \exp(i\vec{k}\cdot(\vec{e}_\circ-\vec{a}_1-\vec{e}_\bullet-\vec{a}_2)) + \exp(i\vec{k}\cdot(\vec{e}_\circ-\vec{a}_2-\vec{e}_\bullet))\Big) + h.c.\,,\end{aligned} \tag{A.3}$$

keeping in mind that $\vec{e}_\circ = -\vec{e}_\bullet$

$$\begin{aligned}\mathbb{H} = t\left(\frac{\sqrt{3}d^2}{8\pi^2}\right) \int_B d^2k\,\tilde{c}_\bullet(\vec{k})^\dagger \tilde{c}_\circ(\vec{k})\Big(\exp(-i\vec{k}\cdot\vec{a}_1) \\ + \exp(-i\vec{k}\cdot(\vec{a}_1+\vec{a}_2)) + \exp(-i\vec{k}\cdot\vec{a}_2)\Big)\exp(-i2\vec{k}\cdot\vec{e}_\bullet) + h.c.\,,\end{aligned} \tag{A.4}$$

introducing $g(\vec{k}) := \Big(\exp(i\vec{k}\cdot\vec{a}_1) + \exp(i\vec{k}\cdot\vec{a}_2) + \exp(i\vec{k}\cdot(\vec{a}_1+\vec{a}_2))\Big)\exp(i2\vec{k}\cdot\vec{e}_\bullet)$

$$\mathbb{H} = t\left(\frac{\sqrt{3}d^2}{8\pi^2}\right) \int_B d^2k\Big(g(\vec{k})^*\tilde{c}_\bullet(\vec{k})^\dagger\tilde{c}_\circ(\vec{k}) + g(\vec{k})\,\tilde{c}_\circ(\vec{k})^\dagger\tilde{c}_\bullet(\vec{k})\Big) \tag{A.5}$$

this can be reinterpreted as

$$\mathbb{H} = t\left(\frac{\sqrt{3}d^2}{8\pi^2}\right) \int_B d^2k \begin{pmatrix}\tilde{c}^\dagger_{s,\bullet} & \tilde{c}^\dagger_{s,\circ}\end{pmatrix}\begin{pmatrix}0 & g^* \\ g & 0\end{pmatrix}\begin{pmatrix}\tilde{c}_{s,\bullet} \\ \tilde{c}_{s,\circ}\end{pmatrix}. \tag{A.6}$$

A unitary transformation yields diagonalization of this matrix ($g = |g|e^{i\alpha}$)

$$U := \frac{1}{\sqrt{2}} \begin{pmatrix} e^{i\frac{\alpha}{2}} & e^{-i\frac{\alpha}{2}} \\ e^{i\frac{\alpha}{2}} & -e^{-i\frac{\alpha}{2}} \end{pmatrix} \quad U^\dagger U = 1 \Longrightarrow$$

$$U \begin{pmatrix} 0 & g^* \\ g & 0 \end{pmatrix} U^\dagger = \frac{1}{2} \begin{pmatrix} e^{i\frac{\alpha}{2}} & e^{-i\frac{\alpha}{2}} \\ e^{i\frac{\alpha}{2}} & -e^{-i\frac{\alpha}{2}} \end{pmatrix} \begin{pmatrix} g^* e^{i\frac{\alpha}{2}} & -g^* e^{i\frac{\alpha}{2}} \\ g e^{-i\frac{\alpha}{2}} & g e^{-i\frac{\alpha}{2}} \end{pmatrix} = \begin{pmatrix} |g| & 0 \\ 0 & -|g| \end{pmatrix} \tag{A.7}$$

and therefore the Hamiltonian in diagonal form reads

$$\mathbb{H} = t \left(\frac{\sqrt{3}d^2}{8\pi^2} \right) \int_B d^2k \begin{pmatrix} \tilde{c}^\dagger_{s,\bullet} & \tilde{c}^\dagger_{s,\circ} \end{pmatrix} U^\dagger \begin{pmatrix} |g| & 0 \\ 0 & -|g| \end{pmatrix} U \begin{pmatrix} \tilde{c}_{s,\bullet} \\ \tilde{c}_{s,\circ} \end{pmatrix}. \tag{A.8}$$

B. Taylor expansions

B.1. Taylor expansion of $|g|$ at the Dirac points $\vec{k}_\pm$

The quantity $|g|$ as a function of k_1 and k_2 takes the form

$$|g(\vec{k})| = \sqrt{3 + 2\cos(dk_1) + 4\cos(\frac{d}{2}k_1)\cos(\frac{d\sqrt{3}}{2}k_2)}, \tag{B.1}$$

and can be expanded around $\vec{k}_\pm$ as

$$\begin{aligned}
|g(\vec{k}_\pm + \Delta\vec{k})| &= \sqrt{3 + 2\cos(\pm\frac{2\pi}{3} + d\Delta k_1) + 4\cos(\pm\frac{\pi}{3} + \frac{d}{2}\Delta k_1)\cos(\mp\pi + d\frac{\sqrt{3}}{2}\Delta k_2)} \\
&= \Big(3 + 2\cos(\frac{2\pi}{3})\cos(d\Delta k_1) \pm 2\sin(\frac{2\pi}{3})\sin(d\Delta k_1) - \\
&\quad 4\cos(\frac{\pi}{3})\cos(\frac{d}{2}\Delta k_1)\cos(d\frac{\sqrt{3}}{2}\Delta k_2) \mp 4\sin(\frac{\pi}{3})\sin(\frac{d}{2}\Delta k_1)\cos(d\frac{\sqrt{3}}{2}\Delta k_2)\Big)^{\frac{1}{2}} \\
&= \Big(3 - \cos(d\Delta k_1) \pm \sqrt{3}\sin(d\Delta k_1) - \\
&\quad 2\cos(\frac{d}{2}\Delta k_1)\cos(d\frac{\sqrt{3}}{2}\Delta k_2) \mp 2\sqrt{3}\sin(\frac{d}{2}\Delta k_1)\cos(d\frac{\sqrt{3}}{2}\Delta k_2)\Big)^{\frac{1}{2}} \\
&= \Big((d\frac{\sqrt{3}}{2}\Delta k_1)^2 + (d\frac{\sqrt{3}}{2}\Delta k_2)^2 \mp \frac{\sqrt{3}}{8}(d\Delta k_1)^3 \pm \\
&\quad d\frac{\sqrt{3}}{2}\Delta k_1(d\frac{\sqrt{3}}{2}\Delta k_2)^2\Big)^{\frac{1}{2}} + \mathcal{O}(\Delta k^3).
\end{aligned} \tag{B.2}$$

By defining $\Delta k_1 = \Delta k\cos(\alpha)$ and $\Delta k_2 = \Delta k\sin(\alpha)$ we obtain

$$\begin{aligned}
|g(\vec{k}_\pm + \Delta\vec{k})| &= \Big((d\frac{\sqrt{3}}{2}\Delta k)^2 \mp \frac{\sqrt{3}}{8}(d\Delta k)^3\cos(3\alpha)\Big)^{\frac{1}{2}} + \mathcal{O}(\Delta k^3) \\
&= \Big(\Big(d\frac{\sqrt{3}}{2}\Delta k \mp \frac{1}{8}(d\Delta k)^2\cos(3\alpha)\Big)^2\Big)^{\frac{1}{2}} + \mathcal{O}(\Delta k^3) \\
&= \frac{\sqrt{3}d}{2}\Delta k \mp \frac{d^2}{8}\cos(3\alpha)\Delta k^2 + \mathcal{O}(\Delta k^3).
\end{aligned} \tag{B.3}$$

B.2. Taylor expansion of $\mathbb{H}$ at the Dirac points $\vec{k}_\pm$

Another way to obtain the result above is to expand the Hamiltonian in a series around $\vec{k}_\pm$

$$\begin{aligned}
g(\vec{k}_\pm + \Delta\vec{k}) =& \left(1 + \exp(-i(\vec{k}_\pm + \Delta\vec{k})\cdot\vec{a}_1) + \exp(-i(\vec{k}_\pm + \Delta\vec{k})\cdot\vec{a}_2)\right) \\
&\times \exp(i(\vec{k}_\pm + \Delta\vec{k})\cdot(2\vec{e}_\bullet + \vec{a}_1 + \vec{a}_2)) \\
=& \left(1 + \exp(-i\vec{k}_\pm\cdot\vec{a}_1)\left[1 - i\Delta\vec{k}\cdot\vec{a}_1\right] + \exp(-i\vec{k}_\pm\cdot\vec{a}_2)\left[1 - i\Delta\vec{k}\cdot\vec{a}_2\right]\right) \\
&\times \exp(i(\vec{k}_\pm + \Delta\vec{k})\cdot(2\vec{e}_\bullet + \vec{a}_1 + \vec{a}_2)) + \mathcal{O}(\Delta k_i^2). \qquad \text{(B.4)}
\end{aligned}$$

Using $\vec{k}_\pm\cdot\vec{a}_1 = \pm\frac{\pi}{3}, \vec{k}_\pm\cdot\vec{a}_2 = \mp\frac{\pi}{3}, \vec{k}_\pm\cdot\vec{e}_\bullet = 0$ gives

$$\begin{aligned}
g(\vec{k}_\pm + \Delta\vec{k}) =& \left(1 + \exp(\mp i\frac{\pi}{3}) + \exp(\pm i\frac{\pi}{3}) - \exp(\mp i\frac{\pi}{3})i\Delta\vec{k}\cdot\vec{a}_1 - \exp(\pm i\frac{\pi}{3})i\Delta\vec{k}\cdot\vec{a}_2\right) \\
&\times \exp(i\Delta\vec{k}\cdot(2\vec{e}_\bullet + \vec{a}_1 + \vec{a}_2)) + \mathcal{O}(\Delta k_i^2) \\
=& - i\Delta\vec{k}\cdot\left(\exp(\mp i\frac{\pi}{3})\,\vec{a}_1 + \exp(\pm i\frac{\pi}{3})\,\vec{a}_2\right) + \mathcal{O}(\Delta k_i^2) \\
=& - i\left(\left[\frac{1}{2} \mp i\frac{\sqrt{3}}{2}\right]\Delta k_1 d + \left[\frac{1}{2} \pm i\frac{\sqrt{3}}{2}\right]\left[\Delta k_1\frac{d}{2} + \Delta k_2\frac{\sqrt{3}d}{2}\right]\right) + \mathcal{O}(\Delta k_i^2) \\
=& \frac{\sqrt{3}d}{2}\left(\left[\mp\frac{1}{2} - i\frac{\sqrt{3}}{2}\right]\Delta k_1 + \left[\pm\frac{\sqrt{3}}{2} - i\frac{1}{2}\right]\Delta k_2\right) + \mathcal{O}(\Delta k_i^2) \\
=& \frac{\sqrt{3}d}{2}\left(\left[\mp\frac{1}{2}\Delta k_1 \pm \frac{\sqrt{3}}{2}\Delta k_2\right] + \left[-i\frac{\sqrt{3}}{2}\Delta k_1 - i\frac{1}{2}\Delta k_2\right]\right) + \mathcal{O}(\Delta k_i^2) \\
=& \frac{\sqrt{3}d}{2}\begin{pmatrix}\pm 1 & i\end{pmatrix}\begin{pmatrix}\cos(\frac{4\pi}{3}) & -\sin(\frac{4\pi}{3}) \\ \sin(\frac{4\pi}{3}) & \cos(\frac{4\pi}{3})\end{pmatrix}\begin{pmatrix}\Delta k_1 \\ \Delta k_2\end{pmatrix} + \mathcal{O}(\Delta k_i^2). \qquad \text{(B.5)}
\end{aligned}$$

Choosing a new basis p_1, p_2 rotated by an angle $\frac{4\pi}{3}$ with respect to $\Delta k_1, \Delta k_2$ yields

$$g_\pm(\vec{p}) = \frac{\sqrt{3}d}{2}\left(\pm p_1 + ip_2\right). \qquad \text{(B.6)}$$

Inserting this into eq. (3.19) gives

$$\mathbb{H}_\pm = v_D\left(\frac{\sqrt{3}d^2}{8\pi^2}\right)\int_B d^2p\begin{pmatrix}\tilde{c}_\bullet^\dagger & \tilde{c}_\circ^\dagger\end{pmatrix}\begin{pmatrix}0 & \pm p_1 - ip_2 \\ \pm p_1 + ip_2 & 0\end{pmatrix}\begin{pmatrix}\tilde{c}_\bullet \\ \tilde{c}_\circ\end{pmatrix} \qquad \text{(B.7)}$$

where we recognize the Dirac Hamiltonian

$$\mathbb{H}_\pm = v_D\left(\pm\sigma_1 p_1 + \sigma_2 p_2\right) \qquad \text{(B.8)}$$

with v_D instead of c and $m = 0$. Applying it twice

$$\mathbb{H}_\pm^2 = v_D^2\left(p_1^2 + p_2^2\right) = v_D^2\,\vec{p}^{\,2} \qquad \text{(B.9)}$$

gives us the same dispersion relation as above

$$E_\pm(\vec{p}) = \pm v_D|\vec{p}|. \qquad \text{(B.10)}$$

References

[1] P. R. Wallace, *The Band Theory of Graphite*, Phys. Rew. 71 622 (1947).

[2] K. S. Novoselov, A. K. Geim, S. V. Morozov, S. V. Dubonos, Y. Zhang, D. Jiang, *Room-temperature electric field effect and carrier-type inversion in graphene films*, Nature, (2004).

[3] A. K. Geim, *Graphene: Status and prospects*, Manchester Centre for Mesoscience and Nanotechnology, University of Manchester, (2005).

[4] J. Fröhlich, U.M. Studer, *Gauge invariance and current algebra in nonrelativistic many-body theory*, Rev. Mod. Phys. 65, (1993).

[5] A. H. Castro Neto, F. Guinea, N. M. R. Peres, K. S. Novoselov and A. K. Geim, *the electronic properties of graphene*, Rev. Mod. Phys., vol. 81, Issue 1, pages 109-162 (2008).

[6] U.-J. Wiese, *Statistical Mechanics*, lecture notes, chapter 15: *Electrons in Solids*, University of Bern, (2010).

[7] C. N. Yang, S. Zhang, *SO(4) symmetry in the Hubbard model*, Mod. Phys. Lett. B4 (1990).

[8] B. Bessire, *Systematic Low-Energy Effective Field Theory for Magnons and Holes in an Antiferromagnet on the Honeycomb Lattice*, arXiv:1109.1419v2 [cond-mat.str-el] (2011).

[9] S. Reich, J. Maultzsch, C. Thomsen, *Tight-binding description of graphene*, Phys. Rev. B 66, 035412, (2002).

[10] F. Kämpfer, M. Moser, U.-J. Wiese, *Systematic low-energy effective theory for magnons and charge carriers in an antiferromagnet*, Nucl. Phys. B729 [FS], pages 317-360, (2005).

[11] V. P. Gusynin, S. G. Sharapov, *Unconventional Integer Quantum Hall Effect in Graphene*, Phys.l Rev. Lett. 95, (2005).

[12] U.-J. Wiese, *Quantum Mechanics*, lecture notes, chapter 6: *The Harmonic Oscillator*, chapter 11: *Particle in an Electromagnetic Field*, University of Bern, (2010).